ELSEVIER

Journal of Organometallic Chemistry 633 (2001) 39–50

Journal of Organometallic Chemistry

www.elsevier.com/locate/jorganchem

Preparation and properties of the halogenoalkyl compounds $[(\eta^5\text{-}C_5H_5)(CO)_2(PPh_iMe_{3-i})Mo\{(CH_2)_nX\}]$ ($n = 3, 4$; $i = 0–3$; X = Br, I) and $[\{\eta^5\text{-}C_5(CH_3)_5\}(CO)_3Mo\{(CH_2)_nX\}]$ ($n = 3, 4$; X = Br, I) and the crystal structures of $[(\eta^5\text{-}C_5H_5)(CO)_3W\{(CH_2)_5I\}]$, $[(\eta^5\text{-}C_5H_5)(CO)_3W\{(CH_2)_3Br\}]$ and $[(\eta^5\text{-}C_5H_5)(CO)_2(PPh_3)Mo\{(CH_2)_3I\}]$

Holger B. Friedrich [a,*], Martin O. Onani [a], Orde Q. Munro [b,*]

[a] *School of Pure and Applied Chemistry, University of Natal, Durban 4041, South Africa*

[b] *School of Chemical and Physical Sciences, University of Natal, Pietermaritzburg, Private Bag X01, Scottsville 3209, South Africa*

Received 2 March 2001; accepted 12 May 2001

Abstract

The compounds $[Cp(CO)_2(PPh_iMe_{3-i})Mo\{(CH_2)_nBr\}]$ ($Cp = \eta^5\text{-}C_5H_5$, $n = 3, 4$; $i = 0–3$) and $[Cp^*(CO)_3Mo\{(CH_2)_nBr\}]$ ($Cp^* = \eta^5\text{-}C_5(CH_3)_5$, $n = 3, 4$) were prepared in medium to high yield by the reaction of the corresponding anion ($[Cp(CO)_2(PPh_iMe_{3-i})Mo]^-$ or $[Cp^*(CO)_3Mo]^-$) with $Br(CH_2)_nBr$. The bromoalkyl compounds were subsequently reacted with NaI to give the corresponding iodoalkyl compounds $[Cp(CO)_2(PPh_iMe_{3-i})Mo\{(CH_2)_nI\}]$ ($n = 3, 4$; $i = 0–3$) and $[Cp^*(CO)_3Mo\{(CH_2)_nI\}]$ ($n = 3, 4$). The iodoalkyl compounds can also be prepared by the reaction of the corresponding anion and α,ω-diiodoalkane in much lower yields. These compounds have been fully characterised and their properties are discussed. The crystal and molecular structure of $[Cp(CO)_2(PPh_3)Mo\{(CH_2)_3I\}]$ is reported. The compound forms crystals in the monoclinic space group $P2_1/n$, with a Mo–C bond length of 2.40 Å and a C–I bond length of 2.13 Å. The compounds $[Cp(CO)_3W\{(CH_2)_nX\}]$ (X = Br, I; $n = 3–6$) were also prepared in high yield and the crystal structures of $[Cp(CO)_3W\{(CH_2)_5I\}]$ and $[Cp(CO)_3W\{(CH_2)_3Br\}]$ are reported. The former compound forms orthorhombic crystals in the space group $P2_1nb$ and the latter forms triclinic crystals in the space group $P\bar{1}$. Both have W–C bond lengths of 2.35 Å. The C–I bond length is 2.12 Å; the C–Br bond length is 1.94 Å. © 2001 Published by Elsevier Science B.V.

Keywords: Haloalkyl ligand; Tungsten; Molybdenum; Carbonyl; Cyclopentadienyl

1. Introduction

Whilst halogenomethyl complexes of several transition metals are fairly well known, longer-chain halogenoalkyl compounds have been comparatively little studied [1]. Indeed, only those of platinum [2], ruthenium [3], iron [4] and, very recently, tungsten [5] have been studied in any detail. Importantly, compounds of the type $[L_yM\{(CH_2)_nX\}]$ (L_yM = transition metal and its associated ligands, $n \geq 1$, X = halogen) are known precursors of cyclic carbene complexes as well as homo- and heterodinuclear compounds (which have been proposed as models for intermediates in several important catalytic processes). The application of several of these compounds in organic synthesis has also been described [1].

Interestingly, although the halogenomethyl compounds $[(\eta^5\text{-}C_5R_5)(CO)_3MoCH_2X]$ (R = H, CH_3; X = Cl, Br, I) are now known [6,7], very few phosphine substituted compounds $[Cp(CO)_2LMoCH_2X]$ (L = tertiary phosphine or phosphite) have been reported. Only

* Corresponding authors. HBF: Tel.: +27-31-260-3107; fax: +27-31-260-3091. OQM (crystallography): Tel.: +27-33-260-5270; fax: +27-33-260-5009..

E-mail addresses: friedric@nu.ac.za (H.B. Friedrich), munroo@nu.ac.za (O.Q. Munro).

0022-328X/01/$ - see front matter © 2001 Published by Elsevier Science B.V.
PII: S0022-328X(01)01044-0

compounds where L = $P(OPh_3)$ and X = Cl, Br and I are known [8]. The only previously reported long-chain halogenoalkyl compounds of molybdenum are $[Cp(CO)_3Mo\{(CH_2)_nX\}]$ ($n = 3$, X = Cl, Br, I; $n = 4$, X = Br, I), $Cp^*(CO)_3Mo\{(CH_2)_3Br\}]$ ($Cp^* = C_5(CH_3)_5$) and $[Cp(CO)_2(PPh_3)Mo\{(CH_2)_3Br\}]$ [9–12]. We now report on the syntheses and properties of the compounds $[Cp(CO)_2(PPh_iMe_{3-i})Mo\{(CH_2)_nX\}]$ ($n = 3$, 4; $i = 0$–3; X = Br, I) and $[Cp^*(CO)_3Mo\{(CH_2)_nX\}]$ ($n =$ 3, 4; X = Br, I) and the structure of $[Cp(CO)_2(PPh_3)$-$Mo\{(CH_2)_3I\}]$. We also report on a new, high-yielding synthetic route to the tungsten analogues, $[Cp(CO)_3W$-$\{(CH_2)_nBr\}]$ ($n = 3$–6), the crystal structure of $[Cp(CO)_3W\{(CH_2)_3Br\}]$ and the crystal structure of $[Cp(CO)_3W\{(CH_2)_5I\}]$. To our knowledge, the latter is the first reported structure of a long-chain halogenoalkyl compound.

2. Results and discussion

Although the bromoalkyl compounds of iron and ruthenium, $[Cp(CO)_2M\{(CH_2)_nX\}]$ (M = Fe, Ru), have to be prepared at low temperature to prevent the formation of the binuclear compounds, $[Cp(CO)_2M$-$(CH_2)_nM(CO)_2Cp]$, these conditions give very low yields for the analogous tungsten and molybdenum compounds, regardless of reaction times. We find that contrary to general expectations, the reaction of $Na[Cp(CO)_3W]$ with excess $Br(CH_2)_nBr$ ($n = 3$–6) under reflux in THF affords the compounds $[Cp(CO)_3W\{(CH_2)_nBr\}]$ in high yield (Eq. (1)), confirming that the anion $[Cp(CO)_3W]^-$ is a significantly weaker nucleophile than the cyclopentadienyldicarbonyl anions of iron and ruthenium [13].

$$Na[(\eta^5\text{-}C_5R_5)(CO)_2LM] + Br(CH_2)_nBr \rightarrow (\eta^5\text{-}C_5R_5)(CO)_2LM\{(CH_2)_nBr\}] + NaBr \quad (1)$$

where M = Mo; $n = 3$, 4; R = H; L = PPh_3, PPh_2Me, $PPhMe_2$, PMe_3; R = CH_3; L = CO. M = W; $n = 3$–6; R = H; L = CO.

Clearly the halogenoalkyl compounds of tungsten are less thermally labile than expected. The dinuclear compounds, $[Cp(CO)_3W(CH_2)_nW(CO)_3Cp]$, are not formed. The compounds, $[Cp(CO)_3W\{(CH_2)_nBr\}]$, are obtained in analytically pure form by recrystallisation from a dilute CH_2Cl_2–hexane solution at −78°C. Analytically pure yields in excess of 90% are obtained by this method, which are some 20% higher than the previously reported method [5]. Chromatography of these compounds, which is essential for the iron analogues [4], is not needed and leads to product loss due to decomposition. The compounds are fairly stable in air in the solid state and are stable in solution under nitrogen, but decompose very rapidly in organic solvents in air. Remarkably, they dissolve in water in air to give stable yellow solutions. The unchanged halogenoalkyl compound can then be recovered. The decomposition product in hexane appears to be the dimer, $[Cp(CO)_3W]_2$, whilst the decomposition products in chloroform include elemental tungsten.

The compounds $[Cp(CO)_2(PPh_iMe_{3-i})Mo\{(CH_2)_n$-$Br\}]$ ($n = 3$, 4; $i = 0$–3) and $[Cp^*(CO)_3Mo\{(CH_2)_nBr\}]$ ($n = 3$, 4) were also prepared by the method shown in Eq. (1), namely by reacting the corresponding anion with the dihalogenoalkane.

The bromoalkyl compounds were then reacted with NaI in acetone at room temperature to give the corresponding iodo compounds, $[Cp(CO)_2LM\{(CH_2)_nI\}]$, in high yield (Eq. (2)).

$$[(\eta^5\text{-}C_5R_5)(CO)_2LM\{(CH_2)_nBr\}] + NaI \rightarrow [(\eta^5\text{-}C_5R_5)(CO)_2LM\{(CH_2)_nI\}] + NaBr \quad (2)$$

where M = Mo; $n = 3$, 4; R = H; L = PPh_3, PPh_2Me, $PPhMe_2$, PMe_3; R = CH_3, L = CO. M = W; $n = 3$–6; R = H; L = CO.

The bromoalkyl compound $[Cp(CO)_2(PPh_3)Mo$-$\{(CH_2)_nBr\}]$, where $n = 3$, has been shown to react with KCN or LiI in refluxing methanol or THF respectively to form the cyclic carbene compounds $[XCp(CO)$-$(PPh_3)Mo\{CO(CH_2)_2CH_2\}]$, X = I, CN [14], thus demonstrating the significant effect of temperature and solvent on the reactions of these haloalkyl compounds, both in terms of yield and in which product is formed. The molybdenum bromoalkyl compounds do, however, form cyclic carbene compounds on reaction with NaI in acetone over longer reaction times (> 24 h). The $[Cp(CO)_3W\{(CH_2)_nI\}]$ compounds have been reported previously [5] and we thus only report data for these compounds, where our data differ significantly from the literature [15].

The molybdenum iodoalkyl compounds could also be obtained by the reaction of the respective anion with $I(CH_2)_nI$, which, after chromatography under N_2, gave analytically pure compounds. Yields, however, are low and the method is not viable.

All compounds (Scheme 1) were obtained as yellow solids or oils. Characterisation data for the compounds are reported in Tables 1–3. From Table 1 it can be seen that the melting points of the compounds decrease steadily as methyl groups sequentially replace phenyl groups in the coordinated tertiary phosphine. The melting points thus decrease with decreasing cone angle and increasing pK_a of the phosphine. The melting points for the compounds where $n = 3$ are higher than those for where $n = 4$. This is as observed for halogenoalkyl iron compounds, as well as for linear unsubstituted paraffins, and can be ascribed to crystal packing factors [16–18]. In the IR spectra, the carbonyl bands move to slightly lower wavenumbers as the halogen changes

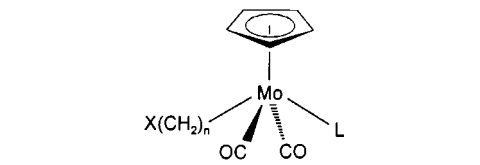

1a L = PPh_3; X = Br; n = 3 **5a** L = $PPhMe_2$; X = Br; n = 3
1b L = PPh_3; X = I; n = 3 **5b** L = $PPhMe_2$; X = I; n = 3
2a L = PPh_3; X = Br; n = 4 **6a** L = $PPhMe_2$; X = Br; n = 4
2b L = PPh_3; X = I; n = 4 **6b** L = $PPhMe_2$; X = I; n = 4
3a L = PPh_2Me; X = Br; n = 3 **7a** L = PMe_3; X = Br; n = 3
3b L = PPh_2Me; X = I; n = 3 **7b** L = PMe_3; X = I; n = 3
4a L = PPh_2Me; X = Br; n = 4 **8a** L = PMe_3; X = Br; n = 4
4b L = PPh_2Me; X = I; n = 4 **8b** L = PMe_3; X = I; n = 4

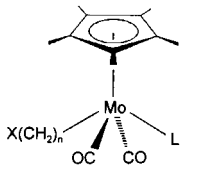

9a L = CO; X = Br; n = 3
9b L = CO; X = I; n = 3
10a L = CO; X = Br; n = 4
10b L = CO; X = I; n = 4

Scheme 1.

Table 1
Data for $[(\eta^5\text{-}C_5R_5)(CO)_2(PPh_iMe_{3-i})Mo\{(CH_2)_n\}X]$, $i = 0$–3, $n = 3$–4

Compound	Yield (%)	m.p. (°C)	IR (ν(CO), cm^{-1}) [a]
1a	57	120–121	1945s, 1868vs
1b	96	>124 dec.	1943s, 1868vs
2a	87	103–105	1941s, 1865vs
2b	92	96–110	1940s, 1865vs
3a	51	98–101	1938s, 1860vs
3b	30	97–99	1938s, 1860vs
4a	40	oil	1935s, 1857vs
4b	46	oil	1935s, 1856vs
5a	54	72–76	1934s, 1856vs
5b	28	74–76	1934s, 1856vs
6a	42	oil	1933s, 1856vs
6b	21	oil	1931s, 1853vs
7a	64	35–39	1935s, 1857vs
7b	29	38–40	1935s, 1857vs
8a	96	oil	1933s, 1855vs
8b	23	oil	1931s, 1854vs
9a	38	84–85	2008s, 1924vs
9b	78	80–82	2007s, 1922vs
10a	18	32–34	2006s, 1919vs
10b	74	34–38	2007s, 1919vs

[a] Measured in hexane.

from Br to I, presumably reflecting the weaker electron withdrawing character of the iodine. As one would expect, the carbonyl bands shift to lower wavenumbers with increasing pK_a of the phosphines, with this effect being more prominent for the compounds where $n = 4$. This is presumably so because the electronegative halogen is further from the metal centres in these latter compounds and hence competes less for electrons. Since the phosphines are *cis* and not *trans* to the carbonyl groups, their effects are relatively small.

The ^{1}H-NMR data for these compounds are shown in Table 2. The MoCH_2 peaks show a small shift with increasing chain length from $n = 3$ to $n = 4$, reflecting the weakening of the inductive effect of the halogen with increasing chain length. An upfield shift of the MoCH_2 peaks is also observed as the pK_a values of the phosphines increase and the cone angles decrease, as would be expected. This effect is more pronounced in the compounds where $n = 4$, because the electronegative halogen is further away. The $\sim$0.2 ppm shift of the CH_2X peaks as X is changed from Br to I is as expected from the difference in their electronegativities. For the compounds where $n = 3$, the peaks also shift slightly upfield with increasing pK_a of the phosphines. This is not observed for the compounds where $n = 4$, presumably because the phosphine is too far away.

Assignments of the ^{13}C-NMR spectra (Table 3) were made using COSY, HMQC and HETCOR experiments. The observation of only a single carbonyl peak (as a doublet) for all the compounds, strongly suggests that the phosphine is *trans* to the alkyl chain, with the two carbonyl groups occupying equivalent *cis* positions. This is confirmed by the crystal structure. Varying the phosphine does not appear to affect significantly the chemical shift of the CO group. Neither the halogen nor the chain length appears to affect greatly the positions of the Cp or carbonyl peaks. There is, however, a trend to lower δ values for the Cp peaks as the cone angle of the phosphine increases and the pK_a increases in going from PPh_3 to PMe_3. This is because the increased electron density increases the shielding of the Cp carbons. The halogen affects the chemical shift of the carbon α to molybdenum. As observed for the iron analogues [4], the peaks due to the α-carbons are shifted upfield for compounds with smaller values of n. This is contrary to what one would expect from consideration of the inductive effects of the halogens and may imply a weak interaction between the halogen and iron, as has been proposed previously [4,12]. The MoCH_2 peaks are at significantly higher field for the iodo compounds than the bromo compounds where $n = 3$, and the opposite effect is observed where $n = 4$. The inverse to the above is observed for the Cp*MoCH_2 peaks. The MoCH_2 peaks also shift to lower field positions with increasing pK_a of the phosphines where X = Br and $n = 3$, whilst the opposite is observed where X = Br, I and $n = 4$. The CH_2I peaks for the compounds where $n = 3$ are at a very much higher field than those are where $n = 4$.

The data above indicate that there are significant differences between the compounds where $n = 3$ and $n = 4$. Specifically, the functionalised ends of the alkyl chain can exert an influence up to a chain length of three carbons, after which negligible or no effect is

Table 2
^{1}H-NMR data for $[(\eta^5\text{-}C_5R_5)(CO)_2(PPh_iMe_{3-i})Mo\{(CH_2)_n\}X]$, $i = 0$–3, $n = 3$–4

Compound	Cp*	Cp	α-CH_2	CH_2X	CH_2CH_2X	β-CH_2	P–Ph	P–CH_3
1a		4.73	1.44	3.37	2.00		7.37	
1b		4.70	1.48	3.15	2.18		7.40	
2a		4.72	1.49	3.40	2.10	1.93	7.39	
2b		4.72	1.49	3.24	2.08	1.90	7.39	
3a		4.71	1.38	3.35	2.11		7.48	2.09
3b		4.71	1.36	3.14	2.10		7.40	2.10
4a		4.71	1.46	3.46	1.89	1.99	7.49	2.11
4b		4.72	1.46	3.25	1.93	1.99	7.39	2.11
5a		4.70	1.33	3.34	1.81		7.41	2.15
5b		4.71	1.33	3.12	1.84		7.42	1.83
6a		4.71	1.36	3.46	1.90	2.01	7.39	1.80
6b		4.71	1.32	3.24	1.92	2.05	7.39	1.82
7a		4.89	1.22	3.32	2.10			1.52
7b		4.88	1.33	3.10	2.12			1.52
8a		4.88	1.32	3.44	1.70	1.88		1.52
8b		4.89	1.32	3.22	1.75	1.86		1.52
9a	1.85		0.81	3.37	2.04			
9b	1.85		0.83	3.14	2.04			
10a	1.84		2.37	3.40	2.01	1.77		
10b	1.84		2.37	3.17	2.01	1.76		

Measured in $CDCl_3$; peaks are externally referenced to TMS ($\delta = 0.00$), α-CH_2 refers to the CH_2-group α to molybdenum etc.

Table 3
^{13}H-NMR data for $[(\eta^5\text{-}C_5R_5)(CO)_2(PPh_iMe_{3-i})Mo\{(CH_2)_n\}X]$, $i = 0$–3, $n = 3$–4

Compound	CO	Cp	Cp*	α-CH_2	CH_2X	CH_2CH_2X	β-CH_2	P–Ph	P–CH_3
1a	237.94	92.72		0.15	37.67	39.54		128.17	
1b	218.49	92.70		2.24	35.85	40.68		128.17	
2a	218.51	92.65		2.23	34.34	30.95	38.77	128.17	
2b	218.43	92.65		1.90	36.79	33.19	39.46	128.10	
3a	236.93	92.38		0.53	39.94	37.63		128.31	21.55
3b	236.93	92.36		2.42	11.93	41.05		128.24	21.54
4a	236.91	92.58		1.73	34.90	34.41	38.99	128.54	21.13
4b	236.95	92.34		1.32	29.69	37.11	39.50	127.69	21.58
5a	236.98	91.83		1.03	37.69	40.17		128.54	20.91
5b	236.94	92.98		1.89	12.09	35.82		128.27	20.43
6a	236.94	91.75		1.07	34.16	34.83	38.82	128.47	20.96
6b	236.95	91.76		1.00	33.79	29.67	39.17	128.29	20.37
7a	235.07	91.02		0.15	37.74	40.39			21.71
7b	236.04	92.21		0.99	18.45	34.50			21.60
8a	237.27	90.96		0.80	35.01	34.20	38.88		21.76
8b	237.46	90.95		1.09	39.64	33.81	39.91		21.78
9a			10.31	8.74	37.81	38.86			
9b	231.26		10.33	0.97	11.48	39.79			
10a			10.31	0.33	36.35	30.87	32.91		
10b			10.54	5.60	25.49	32.54	32.59		

Measured in $CDCl_3$; peaks are externally referenced to TMS ($\delta = 0.00$), α-CH_2 refers to the CH_2-group α to molybdenum etc.

observed. Whether this effect is transmitted through the carbon chain or merely through space is not clear.

The structure of $[Cp(CO)_3W\{(CH_2)_5I\}]$ was determined. The compound forms orthorhombic crystals in the space group $P2_1nb$. The structure of the molecule and packing in the crystal are shown in Figs. 1 and 2. Selected bond lengths and angles for this compound are given in Tables 4 and 5; listings of atomic coordinates, anisotropic temperature factors, H atom coordinates, and complete crystallographic details are given in the supplementary material. In the crystal, the compound shows the classical 'bump in hollow' packing, as is also observed in the packing of paraffins (Fig. 2) [19]. The following (< 4 Å) intermolecular contacts more quantitatively reflect the close packing that is visually evident in Fig. 2: I···O(1), 3.95(2) Å; O(1)···C(8), 3.38(4) Å; O(3)···C(8), 3.64(4) Å; C(p2)···C(6), 3.89(4) Å; C(p3)···C(6), 3.95(1) Å; C(p3)···C(8), 3.91(2) Å;

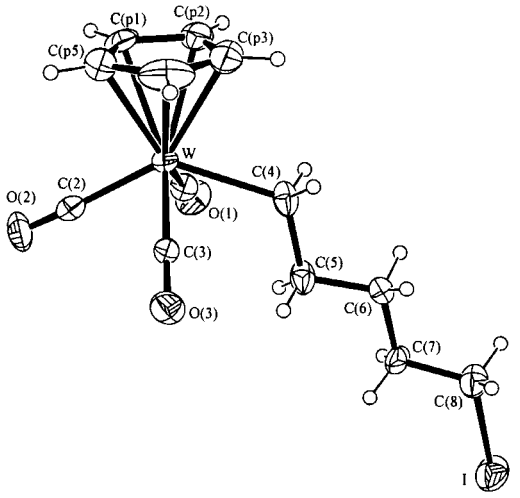

Fig. 1. ORTEP diagram of the X-ray structure of $[Cp(CO)_3W\{(CH_2)_5I\}]$; selected atom labels are shown. Thermal ellipsoids are contoured at the 35% probability level; H atoms have an arbitrary radius of 0.1 Å.

Table 4
Bond distances (Å) for $[Cp(CO)_3W\{(CH_2)_5I\}]$

W–C(3)	1.88(3)	W–C(2)	1.994(10)
W–C(1)	2.08(3)	W–C(p1)	2.347(12)
W–C(p2)	2.373(19)	W–C(p5)	2.307(14)
W–C(4)	2.348(10)	W–C(p3)	2.349(8)
W–C(p4)	2.308(19)	I–C(8) [a]	2.121(10)
O(2)–C(2)	1.140(12)	O(1)–C(1)	1.12(4)
O(3)–C(3)	1.14(3)	C(p1)–C(p2)	1.391(7)
C(p1)–C(p5)	1.391(7)	C(p2)–C(p3)	1.391(7)
C(p3)–C(p4)	1.391(7)	C(p4)–C(p5)	1.391(7)
C(4)–C(5)	1.532(16)	C(5)–C(6)	1.505(11)
C(6)–C(7)	1.507(12)	C(7)–C(8)	1.491(16)

The esds of the least significant digits are given in parentheses.
[a] Symmetry transformation used to generate equivalent atoms: x, $y-1/2$, $-z+5/2$.

C(p4)···C(6), 3.86(4) Å; C(p4)···C(7), 3.98(5) Å; C(p5)···C(6), 3.76(2) Å. As is usual, the alkyl chain lies in an energetically favoured extended staggered conformation (Fig. 1) [20]. While this is true of the ligand conformation, it is noteworthy that the C(2)–W–C(4)–C(5) dihedral angle is nearly eclipsed (9.7°) rather than staggered (180°). This apparently reflects the conformational dictates of facilitating favourable packing of the alkyl chains ('bump in hollow') and the fact that the long W–C bonds that make up the dihedral angle permit a less strained eclipsed configuration than in a simple C–C–C–C dihedral angle. The W–C(4) bond in the alkyl chain was found to be 2.35 Å. To our knowledge, no simple alkyl compounds of the $Cp(CO)_3W$ moiety have been reported, but this bond length is in the general range of reported W–C bonds (2.18–2.36 Å) [21–23], though most of these compounds have different ligands bonded to the metal. The bond length is very similar to that in $[\eta^5\text{-}C_5H_4CH_2\text{-}n\text{-}CH_2)(CO)_3W]$ (2.36 Å), the most similar structure [23].

The structure of $[Cp(CO)_3W\{(CH_2)_3Br\}]$ is similar to that of the iodo compound above; bond lengths and angles for this compound are given in Tables 6 and 7. Complete listings of all crystallographic data for this compound are given in the supplementary material. There are two independent molecules per asymmetric unit; the structure of the molecule and packing in the crystal are shown in Figs. 3 and 4. The W–C bond length of 2.35 Å is identical to the iodo compound above and the C–Br bond of 1.95 Å is within the range found for 'paraffinic' alkyl bromide compounds [24].

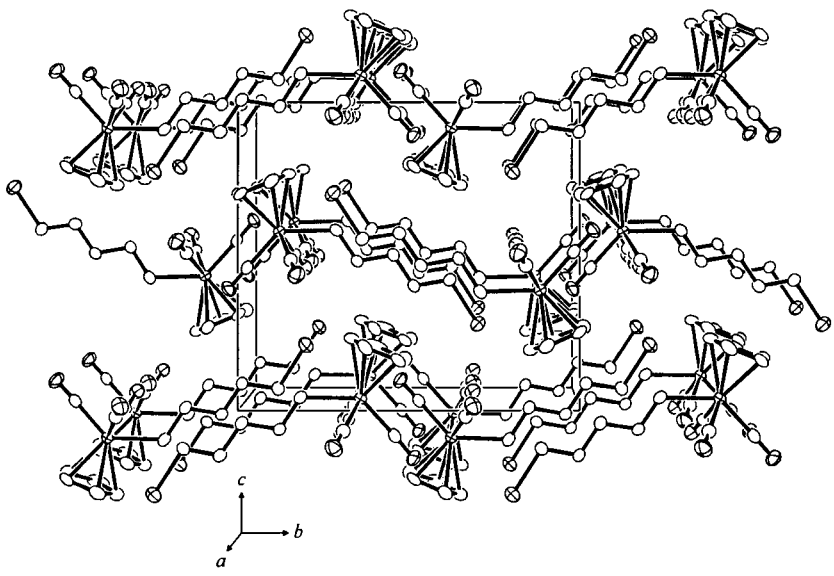

Fig. 2. ORTEP diagram showing the unit cell packing of $[Cp(CO)_3W\{(CH_2)_5I\}]$ viewed down the crystallographic a-axis. Thermal ellipsoids are contoured at the 35% probability level; H atoms have been omitted for clarity.

Table 5
Bond angles (°) for $[Cp(CO)_3W\{(CH_2)_5I\}]$

C(3)–W–C(2)	74.6(11)	C(3)–W–C(1)	106.7(3)
C(2)–W–C(1)	82.3(11)	C(3)–W–C(p1)	147.7(9)
C(2)–W–C(p1)	95.6(6)	C(1)–W–C(p1)	102.2(9)
C(3)–W–C(p2)	150.9(10)	C(2)–W–C(p2)	128.4(8)
C(1)–W–C(p2)	95.2(10)	C(p1)–W–C(p2)	34.3(3)
C(3)–W–C(p5)	113.2(9)	C(2)–W–C(p5)	88.6(5)
C(1)–W–C(p5)	134.9(10)	C(p1)–W–C(p5)	34.76(17)
C(p2)–W–C(p5)	57.5(3)	C(3)–W–C(4)	77.2(12)
C(2)–W–C(4)	133.2(3)	C(1)–W–C(4)	71.0(12)
C(p1)–W–C(4)	126.8(7)	C(p2)–W–C(4)	92.6(7)
C(p5)–W–C(4)	137.2(5)	C(3)–W–C(p3)	116.6(11)
C(2)–W–C(p3)	146.4(4)	C(1)–W–C(p3)	120.0(11)
C(p1)–W–C(p3)	57.3(3)	C(p2)–W–C(p3)	34.3(2)
C(p5)–W–C(p3)	57.8(3)	C(4)–W–C(p3)	80.1(3)
C(3)–W–C(p4)	98.3(10)	C(2)–W–C(p4)	115.9(9)
C(1)–W–C(p4)	152.5(11)	C(p1)–W–C(p4)	57.8(3)
C(p2)–W–C(p4)	57.5(3)	C(p5)–W–C(p4)	35.1(3)
C(4)–W–C(p4)	104.5(7)	C(p3)–W–C(p4)	34.74(19)
C(p2)–C(p1)–C(p5)	108.0	C(p2)–C(p1)–W	73.9(5)
C(p5)–C(p1)–W	71.0(9)	C(p1)–C(p2)–C(p3)	108.0
C(p1)–C(p2)–W	71.9(4)	C(p3)–C(p2)–W	71.9(6)
C(p2)–C(p3)–C(p4)	108.0	C(p2)–C(p3)–W	73.8(8)
C(p4)–C(p3)–W	71.0(8)	C(p5)–C(p4)–C(p3)	108.0
C(p5)–C(p4)–W	72.4(4)	C(p3)–C(p4)–W	74.2(7)
C(p4)–C(p5)–C(p1)	108.0	C(p4)–C(p5)–W	72.5(5)
C(p1)–C(p5)–W	74.2(9)	O(1)–C(1)–W	177(3)
O(2)–C(2)–W	170(4)	O(3)–C(3)–W	179(2)
C(5)–C(4)–W	121.0(8)	C(6)–C(5)–C(4)	112.7(10)
C(5)–C(6)–C(7)	113.9(7)	C(8)–C(7)–C(6)	114.3(9)
C(7)–C(8)–I [a]	113.0(9)		

The esds of the least significant digits are given in parentheses.

[a] Symmetry transformation used to generate equivalent atoms: x, $y+1/2$, $-z+5/2$.

Table 6
Bond distances (Å) for $[Cp(CO)_3W\{(CH_2)_3Br\}]$

W(1)–C(3)	1.949(17)	W(1)–C(1)	1.983(17)
W(1)–C(9)	2.304(17)	W(1)–C(11)	2.326(15)
W(1)–C(4)	2.347(15)	W(1)–C(7)	2.356(16)
W(1)–C(8)	2.362(16)	Br(1)–C(6)	1.946(17)
O(1)–C(1)	1.149(18)	O(2)–C(2)	1.06(2)
O(3)–C(3)	1.17(2)	C(4)–C(5)	1.48(2)
C(5)–C(6)	1.51(2)	C(7)–C(8)	1.39(3)
C(7)–C(11)	1.44(3)	C(8)–C(9)	1.37(3)
C(9)–C(10)	1.39(3)	C(10)–C(11)	1.39(3)
W(2)–C(1b)	1.964(17)	W(2)–C(3b)	2.013(18)
W(2)–C(2b)	2.03(2)	W(2)–C(11b)	2.285(16)
W(2)–C(10b)	2.308(17)	W(2)–C(9b)	2.324(17)
W(2)–C(4b)	2.336(14)	W(2)–C(8b)	2.361(16)
W(2)–C(7b)	2.364(18)	Br(2)–C(6b)	1.941(17)
O(1b)–C(1b)	1.15(2)	O(2b)–C(2b)	1.04(2)
O(3b)–C(3b)	1.118(19)	C(4b)–C(5b)	1.51(2)
C(5b)–C(6b)	1.53(2)	C(7b)–C(8b)	1.40(3)
C(7b)–C(11b)	1.40(3)	C(8b)–C(9b)	1.37(3)
C(9b)–C(10b)	1.40(3)	C(10b)–C(11b)	1.36(3)

The esds of the least significant digits are given in parentheses. Atoms belonging to the second independent molecule in the asymmetric unit (molecule B) are W(2), Br(2), and all those listed with alphanumeric labels containing the letter b.

Table 7
Bond angles (°) for $[Cp(CO)_3W\{(CH_2)_3Br\}]$

C(3)–W(1)–C(1)	106.7(7)	C(3)–W(1)–C(2)	78.9(7)
C(1)–W(1)–C(2)	78.2(6)	C(3)–W(1)–C(10)	144.7(7)
C(1)–W(1)–C(10)	104.1(7)	C(2)–W(1)–C(10)	90.9(7)
C(3)–W(1)–C(9)	152.8(8)	C(1)–W(1)–C(9)	94.9(6)
C(2)–W(1)–C(9)	122.6(8)	C(10)–W(1)–C(9)	35.1(7)
C(3)–W(1)–C(11)	110.5(7)	C(1)–W(1)–C(11)	137.7(7)
C(2)–W(1)–C(11)	89.5(7)	C(10)–W(1)–C(11)	35.0(7)
C(9)–W(1)–C(11)	58.3(7)	C(3)–W(1)–C(4)	72.4(6)
C(1)–W(1)–C(4)	74.6(6)	C(2)–W(1)–C(4)	132.2(6)
C(10)–W(1)–C(4)	133.4(7)	C(9)–W(1)–C(4)	98.4(7)
C(11)–W(1)–C(4)	136.1(7)	C(3)–W(1)–C(7)	98.4(7)
C(1)–W(1)–C(7)	151.3(7)	C(2)–W(1)–C(7)	121.1(7)
C(10)–W(1)–C(7)	58.3(7)	C(9)–W(1)–C(7)	57.3(7)
C(11)–W(1)–C(7)	35.8(7)	C(4)–W(1)–C(7)	100.6(7)
C(3)–W(1)–C(8)	118.8(8)	C(1)–W(1)–C(8)	118.1(7)
C(2)–W(1)–C(8)	146.5(7)	C(10)–W(1)–C(8)	57.8(7)
C(9)–W(1)–C(8)	34.1(7)	C(11)–W(1)–C(8)	58.4(7)
C(4)–W(1)–C(8)	81.3(6)	C(7)–W(1)–C(8)	34.3(7)
O(1)–C(1)–W(1)	176.6(14)	O(2)–C(2)–W(1)	176.4(18)
O(3)–C(3)–W(1)	177.3(17)	C(5)–C(4)–W(1)	116.2(10)
C(4)–C(5)–C(6)	109.0(13)	C(5)–C(6)–Br(1)	113.1(13)
C(8)–C(7)–C(11)	107.6(17)	C(8)–C(7)–W(1)	73.1(9)
C(11)–C(7)–W(1)	70.9(9)	C(9)–C(8)–C(7)	108.1(18)
C(9)–C(8)–W(1)	70.6(10)	C(7)–C(8)–W(1)	72.6(10)
C(8)–C(9)–C(10)	109.4(18)	C(8)–C(9)–W(1)	75.3(10)
C(10)–C(9)–W(1)	72.0(10)	C(9)–C(10)–C(11)	108.6(18)
C(9)–C(10)–W(1)	72.9(10)	C(11)–C(10)–W(1)	73.9(10)
C(10)–C(11)–C(7)	106.2(17)	C(10)–C(11)–W(1)	71.1(9)
C(7)–C(11)–W(1)	73.2(10)	C(1b)–W(2)–C(3b)	106.8(6)
C(1b)–W(2)–C(2b)	77.6(7)	C(3b)–W(2)–C(2b)	77.9(7)
C(1b)–W(2)–C(11b)	111.0(7)	C(3b)–W(2)–C(11b)	137.0(8)
C(2b)–W(2)–C(11b)	90.8(8)	C(1b)–W(2)–C(10b)	144.8(7)
C(3b)–W(2)–C(10b)	103.9(7)	C(2b)–W(2)–C(10b)	92.8(8)
C(11b)–W(2)–C(10b)	34.6(7)	C(1b)–W(2)–C(9b)	152.1(7)
C(3b)–W(2)–C(9b)	95.3(6)	C(2b)–W(2)–C(9b)	124.7(7)
C(11b)–W(2)–C(9b)	57.7(6)	C(10b)–W(2)–C(9b)	35.1(6)
C(1b)–W(2)–C(4b)	72.2(6)	C(3b)–W(2)–C(4b)	75.0(6)
C(2b)–W(2)–C(4b)	130.8(7)	C(11b)–W(2)–C(4b)	136.0(8)
C(10b)–W(2)–C(4b)	133.2(6)	C(9b)–W(2)–C(4b)	98.2(6)
C(1b)–W(2)–C(8b)	118.1(8)	C(3b)–W(2)–C(8b)	119.1(7)
C(2b)–W(2)–C(8b)	147.4(7)	C(11b)–W(2)–C(8b)	57.5(7)
C(10b)–W(2)–C(8b)	57.5(7)	C(9b)–W(2)–C(8b)	34.1(7)
C(4b)–W(2)–C(8b)	81.7(6)	C(1b)–W(2)–C(7b)	97.9(7)
C(3b)–W(2)–C(7b)	152.2(7)	C(2b)–W(2)–C(7b)	120.7(7)
C(11b)–W(2)–C(7b)	35.1(8)	C(10b)–W(2)–C(7b)	57.9(7)
C(9b)–W(2)–C(7b)	57.4(7)	C(4b)–W(2)–C(7b)	101.4(7)
C(8b)–W(2)–C(7b)	34.4(6)	O(1b)–C(1b)–W(2)	177.1(17)
O(2b)–C(2b)–W(2)	179.4(18)	O(3b)–C(3b)–W(2)	177.1(15)
C(5b)–C(4b)–W(2)	116.3(10)	C(4b)–C(5b)–C(6b)	109.2(15)
C(5b)–C(6b)–Br(2)	111.6(13)	C(8b)–C(7b)–C(11b)	105.8(18)
C(8b)–C(7b)–W(2)	72.7(10)	C(11b)–C(7b)–W(2)	69.4(10)
C(9b)–C(8b)–C(7b)	108.8(18)	C(9b)–C(8b)–W(2)	71.5(10)
C(7b)–C(8b)–W(2)	72.9(10)	C(8b)–C(9b)–C(10b)	108.4(17)
C(8b)–C(9b)–W(2)	74.5(10)	C(10b)–C(9b)–W(2)	71.9(10)
C(11b)–C(10b)–C(9b)	107(2)	C(11b)–C(10b)–W(2)	71.8(10)
C(9b)–C(10b)–W(2)	73.1(10)	C(10b)–C(11b)–C(7b)	109.7(18)
C(10b)–C(11b)–W(2)	73.6(10)	C(7b)–C(11b)–W(2)	75.5(11)

The esds of the least significant digits are given in parentheses. Atoms belonging to the second independent molecule in the asymmetric unit (molecule B) are W(2), Br(2), and all those listed with alphanumeric labels containing the letter b.

Whilst the structure clearly shows that there is no bending of the bromine towards the tungsten in the solid state (as possibly indicated in solution), the C(4)–C(5) bond length at 1.48 Å is 0.5 Å shorter than the equivalent bond in the longer chained iodoalkyl compound, which may account for the unusual spectral characteristics of the α-carbons in halogenopropyl compounds. Interestingly, the unit cell packing of $[Cp(CO)_3W\{(CH_2)_3Br\}]$ shown in Fig. 4 reveals that the conformation of the alkyl ligand is probably a compromise between (1) minimizing an unfavourable C(5)···C(8) intramolecular contact between the alkyl and Cp ligands and (2) the reality that 'bump in hollow' packing similar to that of Fig. 2 only becomes more favourable as the alkyl chain becomes longer. The alkyl ligand thus exhibits a C(2)–W(1)–C(4)–C(5) dihedral angle that is closer to 90° than 180° in both independent molecules of the asymmetric unit (119.1 and 118.0° for molecules A and B, respectively).

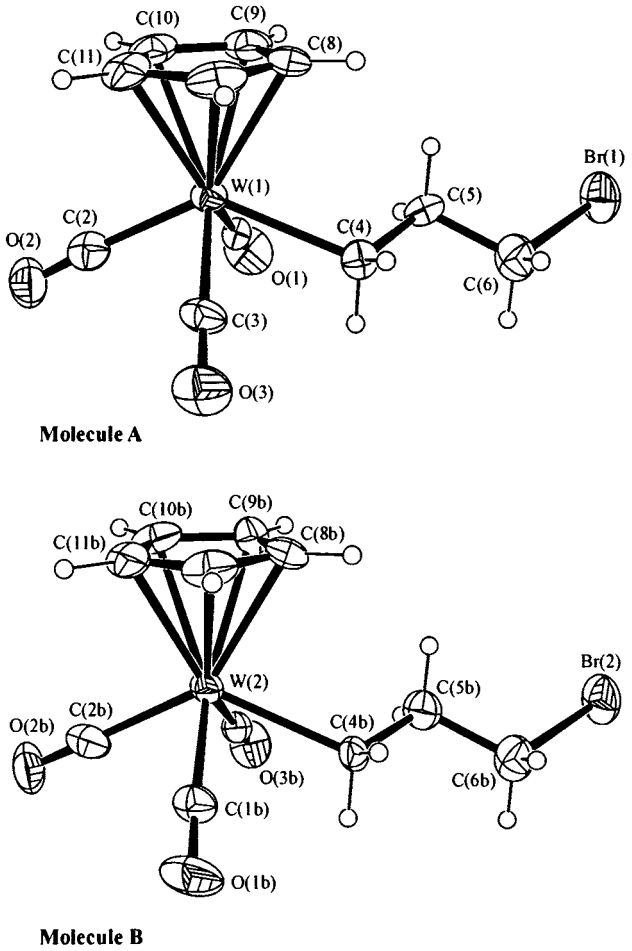

Fig. 3. ORTEP diagrams showing the crystallographically independent molecules (A and B) of the X-ray structure of $[Cp(CO)_3W\{(CH_2)_3Br\}]$; selected atom labels are indicated. Thermal ellipsoids are contoured at the 35% probability level; H atoms have an arbitrary radius of 0.1 Å.

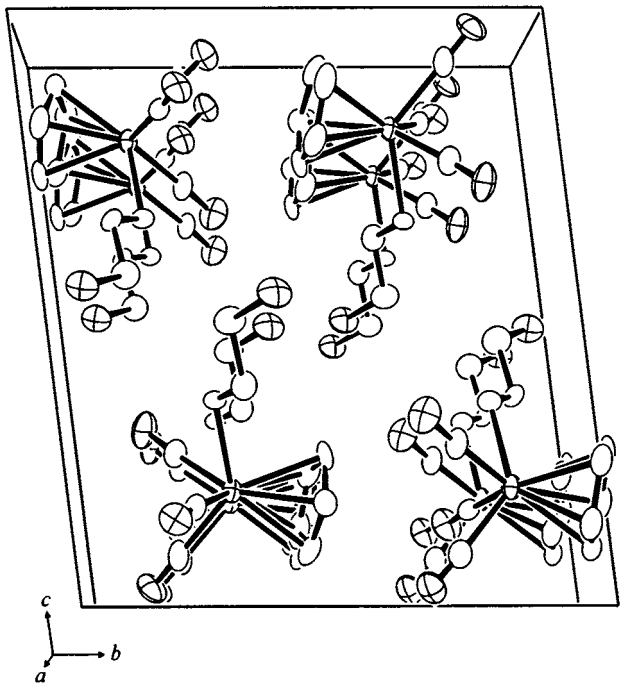

Fig. 4. ORTEP diagram showing the unit cell packing of $[Cp(CO)_3W\{(CH_2)_3Br\}]$ viewed down the crystallographic *a*-axis. Thermal ellipsoids are contoured at the 35% probability level; H atoms have been omitted for clarity.

Table 8
Selected bond distances (Å) for $[Cp(CO)_2(PPh_3)Mo\{(CH_2)_3I\}]$

Mo–C(4)	1.946(7)	Mo–C(5)	1.982(7)
Mo–C(6)	2.318(7)	Mo–C(10)	2.331(7)
Mo–C(7)	2.341(7)	Mo–C(9)	2.342(7)
Mo–C(8)	2.376(7)	Mo–C(1)	2.402(7)
Mo–P	2.4541(17)	I–C(3)	2.134(9)
P–C(17)	1.834(6)	P–C(23)	1.834(6)
P–C(11)	1.840(6)	O(1)–C(4)	1.132(8)
O(2)–C(5)	1.127(8)	C(1)–C(2)	1.264(10)
C(2)–C(3)	1.627(10)	C(6)–C(10)	1.374(11)
C(6)–C(7)	1.380(11)	C(7)–C(8)	1.357(13)
C(8)–C(9)	1.376(13)	C(9)–C(10)	1.402(13)

The esds of the least significant digits are given in parentheses.

Compound **1b** forms crystals in the monoclinic space group $P2_1/n$. Selected bond distances and angles for **1b** are given in Tables 8 and 9; non-hydrogen atomic coordinates, anisotropic temperature factors, H atom coordinates, and complete crystallographic details are given in the supplementary material. The structure of the molecule and packing in the crystal are shown in Fig. 5 and Fig. S1 (supplementary material), respectively. Similar packing to that found for $[Cp(CO)_3W\{(CH_2)_3Br\}]$ (Fig. 4) is observed in the case of compound **1b**. The halogenoalkyl ligand is *trans* to PPh_3 and the P–Mo–C(1)–C(2) dihedral angle is obtuse (110.6°, significantly closer to 90 than 180°). As with $[Cp(CO)_3W\{(CH_2)_3Br\}]$, the 3-carbon alkyl chain

appears to be too short to favour the 'bump in hollow' packing observed for $[Cp(CO)_3W\{(CH_2)_5I\}]$. The C–I bond length of 2.12 Å is within the range of C–I bonds of 'paraffinic' iodoalkyl compounds [24]. The molybdenum to carbon bond in the alkyl chain was found to be 2.40 Å, which is within the range reported for Mo–C (alkyl) bonds (2.27–2.41 Å) [11,25]. Very few structures of molybdenum-alkyl compounds have been reported and to our knowledge none with the $Cp(CO)_2(PR_3)$ ligand pattern. The Mo–C(alkyl) bond lengths of the two $Cp(CO)_3MoR$ compounds previously reported are marginally shorter at 2.36 and 2.38 Å. The Mo–C(carbonyl) bond is also marginally shorter for compound **1b** compared to the Mo–CO bond in the tricarbonyl compounds, indicating the expected greater degree of back-bonding in the PPh_3 substituted compound. No corresponding lengthening of the C–O bond is observed, however, the weakening of this bond is reflected in the comparative IR data. The bond lengths between the alkyl carbons in $[\{Cp(CO)_3Mo\}_2(CH_2)_4]$ are reported as being 1.53 Å [11]. The C(2)–C(3) bond in compound **1b** is rather longer at 1.63 Å, whilst the C(1)–C(2) bond is very short (1.26 Å). However, these values are unlikely to be real and it is likely that they are artifacts due to the large thermal motion of the haloalkyl ligand.

Table 9
Selected bond angles (°) for $[Cp(CO)_2(PPh_3)Mo\{(CH_2)_3I\}]$

C(4)–Mo–C(5)	102.9(3)	C(4)–Mo–C(6)	101.4(3)
C(5)–Mo–C(6)	153.5(3)	C(4)–Mo–C(10)	98.8(3)
C(5)–Mo–C(10)	147.8(3)	C(6)–Mo–C(10)	34.4(3)
C(4)–Mo–C(7)	131.9(3)	C(5)–Mo–C(7)	119.0(3)
C(6)–Mo–C(7)	34.5(3)	C(10)–Mo–C(7)	57.1(3)
C(4)–Mo–C(9)	127.3(3)	C(5)–Mo–C(9)	113.7(3)
C(6)–Mo–C(9)	57.1(3)	C(10)–Mo–C(9)	34.9(3)
C(7)–Mo–C(9)	56.3(3)	C(4)–Mo–C(8)	155.4(3)
C(5)–Mo–C(8)	101.0(3)	C(6)–Mo–C(8)	56.6(3)
C(10)–Mo–C(8)	57.1(3)	C(7)–Mo–C(8)	33.4(3)
C(9)–Mo–C(8)	33.9(3)	C(4)–Mo–C(1)	74.7(3)
C(5)–Mo–C(1)	73.1(2)	C(6)–Mo–C(1)	124.2(3)
C(10)–Mo–C(1)	90.2(3)	C(7)–Mo–C(1)	137.2(3)
C(9)–Mo–C(1)	81.0(3)	C(8)–Mo–C(1)	107.3(3)
C(4)–Mo–P	80.5(2)	C(5)–Mo–P	80.54(17)
C(6)–Mo–P	93.1(2)	C(10)–Mo–P	126.8(2)
C(7)–Mo–P	84.1(2)	C(9)–Mo–P	140.2(2)
C(8)–Mo–P	109.2(3)	C(1)–Mo–P	138.20(18)
C(17)–P–C(23)	103.1(3)	C(17)–P–C(11)	104.0(3)
C(23)–P–C(11)	100.7(3)	C(17)–P–Mo	109.90(19)
C(23)–P–Mo	118.97(18)	C(11)–P–Mo	118.13(19)
C(2)–C(1)–Mo	115.8(5)	C(1)–C(2)–C(3)	113.2(6)
C(2)–C(3)–I	116.9(5)	O(1)–C(4)–Mo	174.9(6)
O(2)–C(5)–Mo	176.8(5)	C(10)–C(6)–C(7)	108.3(7)
C(10)–C(6)–Mo	73.3(4)	C(7)–C(6)–Mo	73.7(4)
C(8)–C(7)–C(6)	108.9(7)	C(8)–C(7)–Mo	74.7(4)
C(6)–C(7)–Mo	71.9(4)	C(7)–C(8)–C(9)	107.9(8)
C(7)–C(8)–Mo	71.8(4)	C(9)–C(8)–Mo	71.7(4)
C(8)–C(9)–C(10)	108.2(7)	C(8)–C(9)–Mo	74.4(4)
C(10)–C(9)–Mo	72.1(4)	C(6)–C(10)–C(9)	106.7(7)
C(6)–C(10)–Mo	72.3(4)	C(9)–C(10)–Mo	73.0(4)

The esds of the least significant digits are given in parentheses.

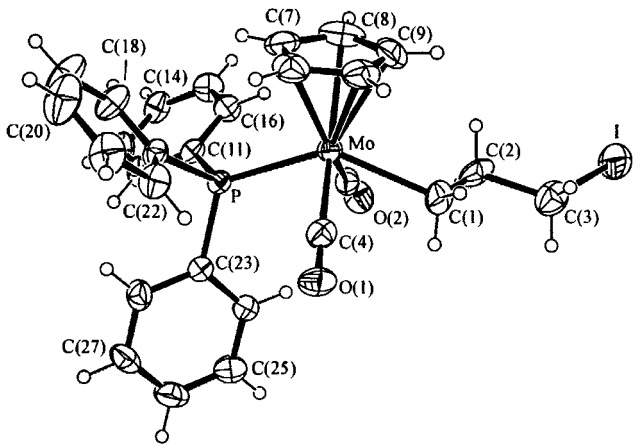

Fig. 5. ORTEP diagram of the X-ray structure of $[Cp(CO)_2(PPh_3)Mo\{(CH_2)_3I\}]$; selected atom labels are shown. Thermal ellipsoids are contoured at the 35% probability level; H atoms have an arbitrary radius of 0.1 Å.

3. Experimental

All reactions were carried out under nitrogen using standard Schlenk tube techniques. Tetrahydrofuran (THF) was distilled from sodium and acetone from anhydrous $CaCl_2$. Hexane and pentamethylcyclopentadiene (Aldrich) were distilled prior to use. $[Cp(CO)_3W]_2$ [26], $[Cp(CO)_2(PPh_3)Mo]_2$, $[Cp(CO)_2(PPh_2Me)Mo]_2$, $[Cp(CO)_2(PPhMe_2)Mo]_2$ [27] and $[Cp^*(CO)_3Mo]_2$] [28] were prepared according to literature procedures with modifications as shown below. The dihaloalkanes, $Mo(CO)_6$, $W(CO)_6$ and the tertiary phosphines (all Aldrich, PMe_3 as the silver iodide salt) were used without further purification and NaI was dried prior to use. Alumina (Merck, active, acidic) was deactivated with deionised water before use. Melting points were recorded on a Kofler hot-stage microscope and are uncorrected. Elemental analyses were performed in the Chemistry Department of our Pietermaritzburg campus or at the SABS in Richards Bay. Infrared spectra were recorded on a Nicolet Impact-400 spectrometer. The NMR spectra were recorded on Varian Unity-Inova 400 and Varian Gemini 300 MHz spectrometers, which also were used for the COSY, HETCOR and HMQC experiments. Solutions for NMR were prepared under nitrogen, using nitrogen saturated solvents.

3.1. Preparation of $[Cp(CO)_3W]_2$

Na (8.6 mmol) was reacted with dicyclopentadiene (11.5 mmol) in N_2-saturated diglyme (34 ml) for 3 h. When all the metal had dissolved, hexacarbonyl tungsten (0.1 mmol) was added and the reaction mixture

refluxed under N_2 (ca. $1\frac{1}{4}$ h). The pink solution turned yellow at the end of the reflux. The product was allowed to cool under N_2 (ca. 45 min). A solution of hydrated ferric sulphate was then prepared under N_2 by dissolving hydrated ferric sulphate (238 mmol) in distilled water (52.5 ml) and acetic acid (3.125 ml). The resulting light pink solution was then slowly added to the reaction solution under N_2 to precipitate the $[Cp(CO)_3W]_2$, which was then filtered off. The filtrate was washed with water (10 ml), methanol (10 ml) and pentane (10 ml) and dried under vacuum overnight. The unreacted hexacarbonyl tungsten was sublimed off the product at 60°C using a cold finger to leave the pure dimer in 91% yield.

3.2. Preparation of $Na[Cp(CO)_3W]$

Na (108 mmol) was reacted slowly with Hg (6 ml) in a Schlenk tube fitted with a bottom tap and the dilute sodium amalgam left to cool to room temperature. THF (30 ml) was added, followed by $[Cp(CO)_3W]_2$ (1.65 mmol). The dimer was reduced to the anion, $[Cp(CO)_3W]^-$ (3.3 mmol), after 2 min of stirring, as shown by a colour change from brick red to green. The mercury was drained off from the bottom of the Schlenk tube.

3.3. Preparation of $[Cp(CO)_3W\{(CH_2)_nBr\}]$, $n = 3–6$

Na $[Cp(CO)_3W]$ (3.3 mmol) in THF (30 ml) was added dropwise over 25 min to a stirred solution of $Br(CH_2)_nBr$ (8.25 mmol) in THF (30 ml) at -25 to -30°C. The solution was then allowed to attain room temperature (ca. 1 h). The mixture was then refluxed under N_2 (using an oil bath at 70°C) for 14 h. The product was allowed to cool to room temperature, filtered through a cannula, and the solvent was then removed under reduced pressure. The product was recrystallised from a mixture of hexane–dichloromethane (10:1) at -78°C. Analytically pure yellow solid was obtained.

3.4. Preparation of $[Cp(CO)_3W\{(CH_2)_nI\}]$, $n = 3–6$

NaI (6.02 mmol) was added to $[Cp(CO)_3W\{(CH_2)_nBr\}]$, $n = 3–6$, (3.01 mmol) in dry, N_2-saturated acetone (10 ml). The solution was stirred at room temperature for 18 h. The solution was filtered through a cannula and the solvent removed under reduced pressure. The yellow solid was recrystallised twice from hexane (40 ml) at -78°C to give the analytically pure product.

3.5. Preparation of dimer $[Cp(CO)_2(PMe_3)Mo]_2$

$[Cp_2(CO)_6Mo_2]$ (9 mmol) and diglyme (12 ml) were used to prepare $[Cp_2(CO)_4Mo_2]$ in situ according to the literature procedure [29]. The mixture was allowed to cool to room temperature under N_2, CH_2Cl_2 (10 ml) was then added and the mixture degassed by several freeze–thaw cycles under vacuum. The mixture was then connected to a U-tube connected to a flask containing the trimethylphosphine silver iodide complex (18 mmol). The trimethylphosphine silver iodide complex was heated slowly and carefully to release a continuous flow of trimethylphosphine gas into the reaction vessel which was maintained in liquid N_2 under vacuum. After all the trimethylphosphine gas had been driven into the reaction vessel, the mixture was allowed to attain room temperature while stirring. Bright red powdered dimer was obtained. The physical properties of the dimers agreed with those in the literature.

3.6. Preparation of $[Cp(CO)_2(PPh_iMe_{3-i})Mo(CH_2)_nBr]$, $i = 0–3$, $n = 3–4$

A solution of $Na[Cp(CO)_2(PPh_iMe_{3-i})Mo]$, $i = 1–3$, (0.477 mmol) in THF (25 ml) prepared by cracking the respective dimers, $[Cp(CO)_2(PPh_iMe_{3-i})Mo]_2$, using Na (152 mmol)–Hg (8 ml) was added over 35 min to a stirred solution of $Br(CH_2)_nBr$ (0.477 mmol) in THF (5 ml) at -25 to -30°C. The solution was stirred for 15 min then allowed to attain room temperature (ca. 4 h), after which the IR spectrum of a sample isolated from the reaction solution no longer showed the ν(CO) stretching frequencies due to the $Na[Cp(CO)_2(PPh_iMe_{3-i})Mo]$. The solvent was removed under reduced pressure, leaving a yellow–black residue. This was extracted with hexane (3×10 ml), and the solution was filtered via a cannula under N_2, concentrated under reduced pressure to approximately a third of the total volume of the hexane used, and then cooled to -78°C under nitrogen (ca. 2 h). The yellow product separated from the solution. The mother liquor was syringed off and the product dried under reduced pressure. Yields and physical properties are listed in Table 1. The residue after the hexane extractions contained small quantities of $[Cp(CO)_2(PPh_iMe_{3-i})MoBr]$ and the respective dimers $[Cp(CO)_2(PPh_iMe_{3-i})Mo]_2$. Anal. Found. (calc.): **3a** C 51.52 (51.20), H 4.8 (4.49); **4a** C 52.07 (52.10), H 4.97 (4.74); **5a** C 44.52 (45.31), H 4.79 (4.65); **6a** C 46.37 (46.46), H 5.04 (4.92); **7a** C 37.98 (37.61), H 4.73 (4.86); **8a** C 38.71 (39.20), H 5.31 (5.17%).

3.7. Preparation of $[Cp(CO)_2(PPh_iMe_{3-i})Mo\{(CH_2)_nI\}]$, $i = 0–3$, $n = 3–4$

NaI (0.300 mmol) was added to a solution of $[Cp(CO)_2(PPh_iMe_{3-i})Mo\{(CH_2)_nBr\}]$ (0.150 mmol) in acetone (12 ml). The solution was stirred at room temperature for 18–24 h, after which the ^{1}H-NMR spectrum of a sample isolated from the reaction solution no longer showed the triplet due to the CH_2Br.

The solvent was removed under reduced pressure, leaving a yellow–orange residue. This was extracted with hexane (3 × 10 ml), and the solution was filtered via a cannula under N_2, concentrated under reduced pressure to approximately a third of the total volume of hexane used and this was then cooled to −78°C under nitrogen. The yellow product separated from the solution. The mother liquor was syringed off and the product dried under reduced pressure. Yields and physical properties are listed in Table 1. The syringed off mother liquor was concentrated and transferred to an alumina column. Elution with 10% CH_2Cl_2–hexane gave an orange band which was identified as $[Cp(CO)_2(PPh_iMe_{3-i})MoI]$ and a dark purple band which contained the respective dimers. Anal. Found (calc.): **3b** C 40.98 (41.24), H 4.09 (4.23); **4b** C 47.16 (48.02), H 4.63 (4.37%).

3.8. Preparation of $[Cp(CO)_2(PPh_iMe_{3-i})Mo\{(CH_2)_nI\}]$ using $I(CH_2)_nI$, $i = 0–3$, $n = 3–4$

A solution of $Na[Cp(CO)_2(PPh_iMe_{3-i})Mo]$ (0.250 mmol, 25 ml THF) was added dropwise into $I(CH_2)_nI$ (0.250 mmol, 5 ml) immersed in a dry ice–acetone bath at −25 to −30°C. The solution was stirred at this temperature for 15 min, after which the mixture was stirred at room temperature until the IR spectrum showed no ν(CO) bands due to the $Na[Cp(CO)_2(PPh_iMe_{3-i})Mo]$. The solvent was removed under reduced pressure, leaving a yellow–orange residue. This was extracted with hexane (3 × 10 ml), and the solution was filtered via a cannula, concentrated under reduced pressure to approximately a third of the total volume of hexane used, and this was then cooled to −78°C under nitrogen. The yellow product separated from the solution. The mother liquor was syringed off and the product dried under reduced pressure. Analytically pure products in very low yields (10–30%) were obtained. Other products observed were identified as $[Cp(CO)_2(PPh_iMe_{3-i})MoI]$ and the respective dimers.

3.9. Preparation of $[Cp^*(CO)_3Mo]_2$

This was prepared according to the literature [28], except that the Cp* was distilled prior to use and all reagents were degassed and all reactions carried out under N_2.

3.10. Preparation of $[Cp^*(CO)_3Mo\{(CH_2)_nBr\}]$, $n = 3–4$

These were prepared using $[Cp^*(CO)_3Mo]_2$ in the same way as $[(\eta^5\text{-}C_5H_5)(CO)_2(PPh_iMe_{3-i})Mo\{(CH_2)_n\text{-}Br\}]$ above, where $i = 0–3$, $n = 3–4$.

3.11. Preparation of $[(\eta^5\text{-}C_5(CH_3)_5)(CO)_3Mo\{(CH_2)_nI\}]$, $i = 0–3$, $n = 3–4$

These were prepared in the same way as the $[(\eta^5\text{-}C_5H_5)(CO)_2(PPh_iMe_{3-i})Mo\{(CH_2)_nI\}]$ compounds above, where $i = 1–3$, $n = 3–4$.

3.12. Single-crystal X-ray diffraction analyses

X-ray data for single crystals of $[Cp(CO)_3W\text{-}\{(CH_2)_5I\}]$, $[Cp(CO)_3W\{(CH_2)_3Br\}]$ and $[Cp(CO)_2\text{-}(PPh_3)Mo\{(CH_2)_3I\}]$ were collected on an Enraf–Nonius CAD4 diffractometer at 20(2)°C using Mo–K_α wavelength radiation (0.70930 Å). The data were reduced with the program XCAD [30]. Semi-empirical absorption corrections were applied to the data for the two iodo derivatives using a minimum of four reflections with χ-values $> 75°$ (azimuthal ψ-scan method) with the program ABSCALC, as implemented in OSCAIL [30]. The data for the bromo derivative were corrected for absorption using the Fourier series method of DIFABS [31]. The structure of $[Cp(CO)_3W\{(CH_2)_5I\}]$ was solved in the orthorhombic space group $P2_1nb$ with the direct methods program SHELXS-97 [32]. The structures of $[Cp(CO)_3W\text{-}\{(CH_2)_3Br\}]$ and $[Cp(CO)_2(PPh_3)Mo\{(CH_2)_3I\}]$ were solved in the triclinic and monoclinic space groups $P\bar{1}$ and $P2_1/n$, respectively, with the direct methods program DIRDIF [33], as implemented by the crystallographic program WinGX [34]. In each case, the final model was plotted with Farrugia's 32-bit implementation of the program ORTEP [35]. Crystal data, lattice constants, and least-squares refinement details for the three compounds are listed in Table 10.

4. Supplementary material

Crystallographic data for the structural analyses have been deposited with the Cambridge Crystallographic Data Centre, CCDC nos. 158285 for $[Cp(CO)_3W\{(CH_2)_5I\}]$, 158286 for $[Cp(CO)_3W\{(CH_2)_3\text{-}Br\}]$ and 158287 for $[Cp(CO)_2(PPh_3)Mo\{(CH_2)_3I\}]$. Copies of this information may be obtained free of charge from The Director, CCDC, 12 Union Road, Cambridge, CB2 1EZ, UK (Fax: +44-1223-336033; e-mail: deposit@ccdc.cam.ac.uk or www: http://www.ccdc.cam.ac.uk). Full tables of crystallographic data (crystallographic details, atomic coordinates, thermal parameters, bond distances and bond angles) for $[Cp(CO)_3W\{(CH_2)_5I\}]$, $[Cp(CO)_3W\{(CH_2)_3Br\}]$ and $[Cp(CO)_2(PPh_3)Mo\{(CH_2)_3I\}]$ (21 pages) are also available from the authors.

Table 10
Crystallographic data for $[Cp(CO)_3W\{(CH_2)_5I\}]$, $[Cp(CO)_3W\{(CH_2)_3Br\}]$ and $[Cp(CO)_2(PPh_3)Mo\{(CH_2)_3I\}]$

	$[Cp(CO)_3W\{(CH_2)_5I\}]$	$[Cp(CO)_3W\{(CH_2)_3Br\}]$	$[Cp(CO)_2(PPh_3)Mo\{(CH_2)_3I\}]$
Empirical formula	$C_{13}H_{15}IO_3W$	$C_{11}H_{11}BrO_3W$	$C_{28}H_{26}IMoO_2P$
Formula weight (g mol^{-1})	530.00	454.96	648.30
Crystal system, space group	Orthorhombic, $P2_1nb$	Triclinic, $P\bar{1}$	Monoclinic, $P2_1/n$
Unit cell dimensions			
a (Å)	8.3227(9)	6.8337(14)	17.4796(12)
b (Å)	14.0192(16)	12.896(4)	9.2587(13)
c (Å)	12.5856(13)	14.355(3)	17.558(3)
α (°) [a]		97.13(2)	
β (°) [a]		89.995(18)	112.66(9)
γ (°) [a]		90.08(3)	
Volume (Å^3), Z	1468.5(3), 4	1255.3(5), 4	2622.2(6), 4
D_{calc} (g cm^{-3})	2.397	2.407	1.642
Absorption coefficient (mm^{-1})	9.966	12.374	1.761
Crystal size (mm), colour	$0.20\times0.15\times0.15$, yellow	$0.35\times0.25\times0.15$, orange	$0.65\times0.40\times0.20$, orange–red
θ range for data collection (°)	2.17–22.97	2.00–24.97	2.10–22.97
Index ranges	$-2\le h\le9$, $-5\le k\le15$, $-13\le l\le13$	$-8\le h\le8$, $-15\le k\le15$, $0\le l\le17$	$-5\le h\le19$, $-4\le k\le10$, $-19\le l\le18$
Reflections collected, unique	3181, 1409 [$R_{int}=0.0261$]	4397, 4397 [$R_{int}=0.0000$] [b]	5606, 3629 [$R_{int}=0.0229$]
Reflections observed ($>2\sigma$)	1219	3025	3180
Maximum and minimum transmission	0.3164, 0.2405	0.2583, 0.0982	0.7196, 0.3940
Goodness-of-fit on F^2	1.036	1.052	1.106
Final R indices [$I>2\sigma(I)$] [c]	$R_1=0.0234$, $wR_2=0.0615$	$R_1=0.0493$, $wR_2=0.1236$	$R_1=0.0464$, $wR_2=0.1411$
R indices (all data) [c]	$R_1=0.0295$, $wR_2=0.0642$	$R_1=0.0851$, $wR_2=0.1348$	$R_1=0.0518$, $wR_2=0.1459$
Residual extrema (e Å^{-3})	0.547, −0.893	2.213, −1.368	1.336, −1.596

The esds of the least significant digits are given in parentheses.
[a] Crystallographically required 90° angles are not given.
[b] Internal R-factor before DIFABS [31] absorption correction 0.0194.
[c] $R_1=\Sigma(||F_o|-|F_c||)^2/\Sigma|F_o|$; $wR_2=(\Sigma[w(F_o^2-F_c^2)^2]/\Sigma[wF_o^4])^{0.5}$. R-factors R_1 are based on F, with F set to zero for negative F^2. The criterion of $F^2>2\sigma(F^2)$ was used only for calculating R_1. R-factors based on F^2 (wR_2) are statistically about twice as large as those based on F.

Acknowledgements

We thank the University of Natal (URF), the National Research Foundation, Pretoria (NRF) and the Deutscher Akademischer Austausch Dienst (DAAD) for financial support. MOO thanks the DAAD for a Ph.D. scholarship and the Jomo Kenyatta University of Agriculture and Technology (Nairobi) for study leave. OQM thanks James Ryan for mounting and taking preliminary X-ray photographs of several crystal specimens relevant to this work. Finally, we thank Professor M. Laing for useful discussions of the crystal data.

References

[1] H.B. Friedrich, J.R. Moss, Adv. Organomet. Chem. 33 (1991) 235.
[2] P.K. Monaghan, R.J. Puddephatt, J. Chem. Soc. Dalton Trans. (1988) 595.
[3] H.B. Friedrich, K.P. Finch, M.A. Gafoor, J.R. Moss, Inorg. Chim. Acta 206 (1993) 225.
[4] H.B. Friedrich, P.A. Makhesha, J.R. Moss, B.K. Williamson, J. Organomet. Chem. 384 (1990) 325.
[5] X. Yin, J.R. Moss, J. Organomet. Chem. 574 (1999) 252.
[6] M.L.H. Green, M. Ishaq, R.N. Whiteley, J. Chem. Soc. A (1967) 1508.
[7] R.B. King, D.M. Braitsch, J. Organomet. Chem. 54 (1973) 9.
[8] D.H. Gibson, S.K. Mandal, K. Owen, W.E. Sattich, J.O. Franco, Organometallics 8 (1989) 1114.
[9] R.B. King, M.B. Bisnette, J. Organomet. Chem. 7 (1967) 311.
[10] N.A. Bailey, D.A. Dunn, C.N. Foxcroft, G.R. Harris, M.J. Winter, S. Woodward, J. Chem. Soc. Dalton Trans. (1988) 1449.
[11] H. Adams, N.A. Bailey, M.J. Winter, J. Chem. Soc. Dalton Trans. (1984) 273.
[12] C.P. Casey, L.J. Smith, Organometallics 7 (1988) 2419.
[13] R.B. King, Acc. Chem. Res. 3 (1970) 417.
[14] N.A. Bailey, P.L. Chell, C.P. Manuel, A. Mukhopadhyay, D. Rodgers, H.E. Tabron, M.J. Winter, J. Chem. Soc. Dalton Trans. (1983) 2397.
[15] $[Cp(CO)_3W\{(CH_2)_4Br\}]$: m.p. = 66–67°C. $[Cp(CO)_3W\{(CH_2)_4I\}]$: m.p. = 109–110°C. $[Cp(CO)_3W\{(CH_2)_6Br\}]$: m.p. = 61–63°C. $[Cp(CO)_3W\{(CH_2)_6I\}]$: m.p. = 64–66°C. ^{13}C-NMR ($CDCl_3$) δ = 220.44 (CO), 94.32 (Cp), 39.47 (βCH_2), 37.61 (γCH_2), 36.44 (δCH_2), 32.85 (CH_2CH_2I), −7.59 (CH_2I).
[16] L. Pope, P. Somerville, M.J. Laing, K.J. Hindson, J.R. Moss, J. Organomet. Chem. 112 (1976) 309.
[17] R. Boese, H.-C. Weiss, D. Bläser, Angew. Chem. Int. Ed. Engl. 38 (1999) 988.
[18] A.P. Malanoski, P.A. Monson, J. Chem. Phys. 110 (1999) 664.
[19] A.I. Kitaigorodskii, Organic Chemical Crystallography, Consultants Bureau, New York, 1961, p. 65.
[20] R.O. Hill, C.F. Marais, J.R. Moss, K.J. Naidoo, J. Organomet. Chem. 587 (1999) 28.
[21] D.J. Darensbourg, R. Kudaroski, J. Am. Chem. Soc. 106 (1984) 3672.
[22] D.J. Debad, P. Legzdins, S.J. Rettig, J.E. Veltheer, Organometallics 12 (1993) 2714.

[23] F. Amor, P. Royo, T.P. Spaniol, J. Okuda, J. Organomet. Chem. 604 (2000) 126.
[24] A.I. Kitaigorodskii, Organic Chemical Crystallography, Consultants Bureau, New York, 1961, p. 3.
[25] M.R. Churchill, S.W.-Y. Chang, Inorg. Chem. 14 (1975) 99.
[26] R. Birdwhistell, P. Hacket, A.R. Manning, J. Organomet. Chem. 157 (1978) 239.
[27] N. Chip, J.A. Robert, Inorg. Chem. 37 (1998) 2975.
[28] M. Fei, S.K. Sur, D.R. Tyler, Organometallics 10 (1991) 419.
[29] M.D. Curtis, M.S. Hay, Inorg. Synth. 28 (1990) 150.
[30] P. McArdle, OSCAIL, Version 8, Crystallography Center, Chemistry Department, NUI Galway, Ireland. P. McArdle, J. Appl. Crystallogr. 28 (1995) 65.
[31] N. Walker, D. Stuart, DIFABS, Acta Crystallogr. Sect. A 39 (1983) 158.
[32] G.M. Sheldrick, SHELXL-97, University of Göttingen. (a) G.M. Sheldrick, Acta Crystallogr. Sect. A 46 (1990) 467. (b) G.M. Sheldrick, Acta Crystallogr. Sect. D 49 (1993) 18. (c) G.M. Sheldrick, T.R. Schneider, Methods Enzymol. 277 (1997) 319.
[33] P.T. Beurskens, G. Beurskens, W.P. Bosman, R. de Gelder, S. Garcia-Granda, R.O. Gould, R. Israel, J.M.M. Smits, DIRDIF96, Crystallography Laboratory, University of Nijmegen, The Netherlands. 1996.
[34] L.J. Farrugia, WinGX: A Windows Program for Crystal Structure Analysis, University of Glasgow, Glasgow, 1998.
[35] (a) L.J. Farrugia, ORTEP3 for Windows V1.01 beta, Department of Chemistry, University of Glasgow, Glasgow, 1998;
(b) M.N. Burnett, C.K. Johnson, ORTEP III, Oak Ridge National Laboratory Report ORNL-6895, Oak Ridge, TN, 1996.